Molecular Neurobiology (2019) 56:5136–5145
https://doi.org/10.1007/s12035-018-1438-5

# Attenuation of Experimental Autoimmune Encephalomyelitis in a Common Marmoset Model by Dendritic Cell-Modulating Anti-ICAM-1 Antibody, MD-3

Soon-Tae Lee[1] · Seung Pyo Park[2] · Hi-Jung Park[3] · Joan R. Wicks[4] · Jae-Il Lee[3,5,6] · Young Ho Suh[2,7] · Kyeong Cheon Jung[3,5,8]

Received: 2 August 2018 / Accepted: 20 November 2018 / Published online: 28 November 2018


## Abstract

MD-3 is a novel anti-human ICAM-1 monoclonal antibody that induces T cell tolerance in humanized mice via modulation of dendritic cell differentiation and efficiently suppresses the development of collagen-induced arthritis. This effect has also been observed in xenograft rejection in nonhuman primates, where grafts survived for more than 2.5 years following MD-3 administration. Here, we show that MD-3 can attenuate experimental autoimmune encephalomyelitis (EAE) that was induced in common marmoset monkeys by immunization with human myelin oligodendrocyte glycoproteins. MD-3 administration was initiated 1 week after immunization and efficiently delayed the development of EAE phenotypes, although the disease was not completely prevented. Based on the results of histopathological examination, MD-3 treatment greatly suppressed total inflammation with respect to demyelination, as well as T cell and microglial infiltration in the brain. However, the antibody response against myelin oligodendrocyte glycoprotein was not suppressed with this treatment protocol. These observations suggest that the MD-3 antibody has beneficial effects on the treatment of EAE via the suppression of T cell-mediated cellular responses.

**Keywords** Autoimmunity · Experimental autoimmune encephalomyelitis · MD-3 · Anti-ICAM-1 antibody

## Introduction

Multiple sclerosis (MS) is a prototypical autoimmune disease characterized by multifocal demyelinating brain lesions disseminated in time or space and can be categorized into several clinical phenotypes, namely isolated syndrome, relapsing-remitting type, primary/secondary progressive types, and progressive relapsing type [1, 2]. Pathologically, the infiltration of myelin-reactive T cells and macrophages coupled with damaged blood-brain barriers is found in MS plaque lesions. A number of previous observations reported that these phenomena are induced by Th1- and Th17-type immune activation [3, 4]. Immunization with myelin antigens, such as myelin oligodendrocyte glycoprotein (MOG), evokes experimental autoimmune encephalitis (EAE) in rodents and nonhuman primates to create animal models of MS [5]. Similar to other autoimmune diseases, the activated Th1 and Th17 cells are initiated by dendritic cells in MS and EAE [6], and tissue damage is responsible for epitope spreading with a variety of autoreactive T cell clones, finally leading to relapsing-remitting and progressive disease patterns [7–9]. Accordingly, the inhibition of dendritic cell maturation, T

Soon-Tae Lee and Seung Pyo Park contributed equally to this work.

✉ Kyeong Cheon Jung
jungkc66@snu.ac.kr

[1] Department of Neurology, Seoul National University Hospital, Seoul, Republic of Korea

[2] Neuroscience Research Institute, Seoul National University Medical Research Center, Seoul, Republic of Korea

[3] Graduate Course of Translational Medicine, Seoul National University College of Medicine, Seoul, Republic of Korea

[4] Alizée Pathology, Thurmont, MD 21788, USA

[5] Transplantation Research Institute, Seoul National University Medical Research Center, Seoul, Republic of Korea

[6] Department of Medicine, Seoul National University College of Medicine, Seoul, Republic of Korea

[7] Department of Biomedical Sciences, Seoul National University College of Medicine, Seoul, Republic of Korea

[8] Department of Pathology, Seoul National University College of Medicine, 103 Daehak-ro, Jongno-gu, Seoul 03080, Republic of Korea

cell infiltration, and clonal spreading would be key targets for the control of EAE or MS [7, 8].

ICAM-1 is a representative adhesion molecule involved in leukocyte-endothelial adhesion, leukocyte migration, and interactions between T cells and antigen-presenting cells via binding to LFA-1 or MAC-1. Consequently, anti-human ICAM-1 blocking antibodies, such as R6-5-D6 (BIRR-1, Enlimomab), were developed as anti-inflammatory agents to control autoimmune diseases, transplant rejection, and stroke [10–12]. R6-5-D6 was initially demonstrated to have beneficial effects in reducing diseased activity in rheumatoid arthritis patients [11]. However, interfering with leukocyte migration potentially increases susceptibility to infection and leukopenia, impeding the clinical application of the R6-5-D5 antibody [13].

MD-3 is another type of anti-human ICAM-1 monoclonal antibody that modulates immune responses with a novel mode of action compared to other conventional anti-ICAM-1 blocking antibodies [14]. MD-3 induces T cell tolerance in situ via modulation of dendritic cell differentiation without inhibiting leukocyte-endothelial adhesion. Notably, MD-3 treatment in diabetic monkeys transplanted with porcine islet facilitated long-term survival of the xenografts without severe adverse effects [14, 15]. Additionally, MD-3 treatment efficiently suppressed the development of collagen-induced arthritis (CIA) [16]. The primary goal of this study is to investigate the therapeutic efficacy of MD-3 in EAE in nonhuman primates.

## Materials and Methods

### Animals

The animal study was performed in Biomere (Worcester, MA, USA) in accordance with the Guide for the Care and Use of Laboratory Animals of the USA National Institutes of Health and approved by the Institutional Animal Care and Use Committee (IACUC) of the Testing Facility (permission number 15-16). Ten male common marmosets (*Callithrix jacchus*) were selected from the Testing Facility colony. Animals were enrolled after complete physical, hematological, and biochemical check-ups had been performed. During the study, animals were housed individually or in pairs. Study animals were fed a special diet designed to provide nutrition and enrichment. This is the standard diet provided to the Testing Facility marmoset colony. Filtered tap water was provided ad libitum. To our knowledge, there were no contaminants in the feed and water that would interfere with the objectives of the study.

### Induction of EAE

EAE was induced by immunization with recombinant human $MOG_{1–125}$ ($rhMOG_{1–125}$) protein as previously described [17]. Ten unrelated male common marmosets were randomly assigned to the vehicle or MD-3-treated groups ($n = 5$ per group). On day 1, all animals were immunized with a single intradermal administration containing 100 μg of $rhMOG_{1–125}$ (AnaSpec, Fremont, CA, USA) emulsified in complete Freund's adjuvant split into two spots on the back at a total volume of 200 μL/animal (Fig. 1a). On days 8, 11, and 15 and once weekly thereafter, animals received either an intravenous injection of vehicle (*phosphate-buffered saline, PBS)* or MD-3 antibody (8 mg/kg). Animal health checks were performed at least once daily, in which all animals were checked for general health, mortality, and morbidity. Clinical scoring was performed twice daily beginning on day 1. Each animal was assessed for physical appearance and disability as follows: 0 = no clinical sign; 0.5 = apathy, loss of appetite, vomiting, and altered walking without ataxia; 1 = lethargy, anorexia, tail paralysis, and tremor; 2 = ataxia and optic disease (vision problems); 2.5 = monoparesis or paraparesis, sensory loss, and brainstem syndrome; 3 = hemiplegia or paraplegia; 4 = quadriplegia; and 5 = moribund or spontaneous death attributable to EAE. Body weights were recorded before immunization and two to three times weekly thereafter. Humane endpoints included progression to a clinical score of ≥ 2.5 or ≥ 20% body weight loss, which served as a surrogate marker for acute onset disease [18] or per veterinarian recommendation.

### Magnetic Resonance Imaging Studies

Magnetic resonance imaging (MRI) studies were performed at Northeastern University Center for Translational Neuro-Imaging (Boston, MA, USA), when an animal reached or was expected to reach a humane endpoint. On the day of imaging, the animal was assessed for general health, scored, and then transported to the imaging center at Northeastern University by a Testing Facility veterinarian and a research technician or study director. If an animal was deemed by the veterinarian to be too unhealthy enough for transport and anesthetization, then no imaging was attempted. Imaging was performed on anesthetized animals using a Bruker BioSpec 70/20 instrument (Bruker BioSpec, Ettlingen, Germany), and T1-weighted, T2-weighted, and DTI images were captured and analyzed. For volumetric analysis of MRI, white matter was segmented according to fractional anisotropy, and the lesion was discriminated based on the T2 intensity. At the beginning of each imaging session, a high-resolution T1- and T2-weighted anatomical data set was collected using the RARE pulse sequence (40 slices; 0.8 mm slice thickness; field of view [FOV] 3.5 cm; 256 × 256 in-plane resolution). For T1-weighted images, the echo time (TE) was 9 ms and the repetition time (TR) was 1200 ms. For T2-weighted images, the effective TE was 48 ms and TR was 4500 ms. The anatomy scans were followed by diffusion-weighted imaging (DWI) scans. The white matter was segmented using MRI

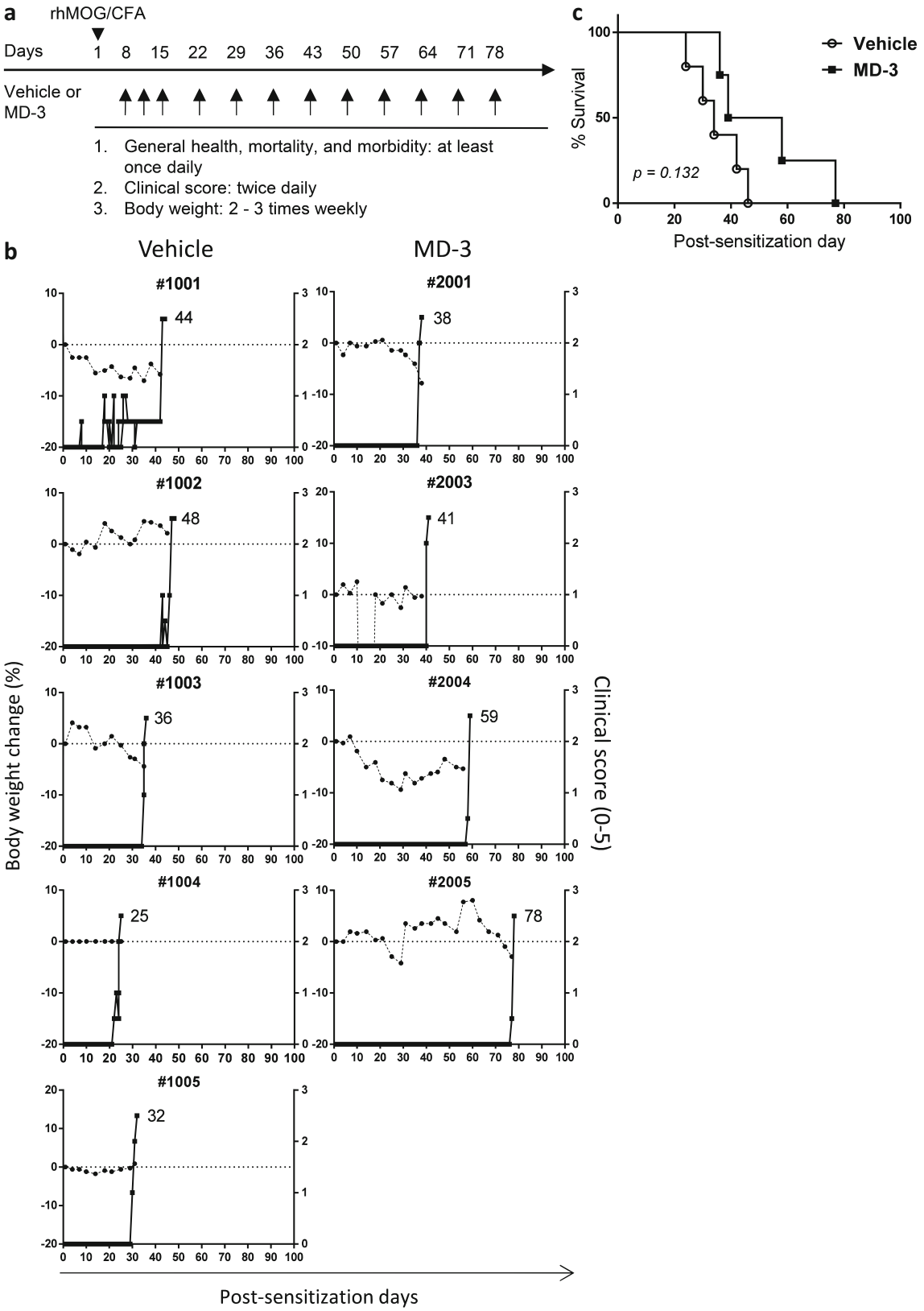


**Fig. 1** MD-3 treatment delayed the development of EAE in marmosets. **a** EAE experiment scheme. **b** Body weight loss and clinical score of vehicle or MD-3-treated rhMOG-immunized marmosets. Body weight change in percentages compared with day 1 (dotted line, left *y*-axis) and clinical scores (solid line, right *y*-axis) for the vehicle (left panels) and MD-3-treated (right panels) groups are presented. Numbers in the figures represent the day of euthanasia. **c** Survival time to day of euthanasia is compared between the vehicle and MD-3-treated marmosets. The MD-3 treated group showed a longer survival curve, although the difference was not statistically significant

Marmoset Brain atlas (Ekam Solutions LLC, Boston, MA, USA) and T1-weighted MR images. The lesions were identified and segmented using T2-weighted images in itk-SNAP (http://www.itksnap.org/) software. An active contour segmentation model (snake algorithm) in itk-SNAP software [19] with the region competition force $\alpha = 1$ and smoothing force $\beta = 0.2$ was used to segment white matter lesions. The segmentation was checked slice by slice and corrected manually if necessary. The integral summations of each lesion area were compared between the two treatment groups.

## Postmortem Examination

If selected for necropsy, monkeys were first deeply sedated by intramuscular injection of ketamine (15–40 mg/kg) and subsequently euthanized by the infusion of Euthasol (≥ 50 mg/kg). The brain and spinal cord were harvested at euthanasia and a portion of each was fixed in 10% neutral buffered formalin for histopathological and immunohistochemical analysis.

## Histopathological and Immunohistochemical Analysis

Fixed brain and spinal cord samples were embedded in paraffin, sectioned, and stained with hematoxylin and eosin and Luxol fast blue, followed by immunohistochemical analysis with anti-CD3 and MRP-14 antibodies. Microscopic evaluation of the tissue response to treatment was performed by a study pathologist at Alizée Pathology LLC (Thurmont, MD, USA). Samples were evaluated in particular for the following: total inflammation/gliosis, inflammatory cuffing, activated microglial cells (MRP-14-positive), demyelination, and the percentage of $CD3^+$ and MRP-$14^+$ cells in cuffs and in parenchyma. Scoring definitions for the parameters evaluated are provided in Table 1. After the whole evaluation is finalized, the groups are sorted separately and independent of the pathologist by support staff.

## Real-Time Quantitative PCR

Total mRNA were extracted from the marmoset cerebral hemisphere using TRIzol (Invitrogen, Carlsbad, CA, USA), chloroform (Merck, Darmstadt, Germany), and isopropanol (Sigma, St. Louis, MO, USA). cDNA was subsequently made using Accupower CycleScript RT Premix with oligo (dT)20 (Bioneer, Daejeon, Korea) according to the manufacturer's instructions. Real-time quantitative PCR (RT-qPCR) was performed as described previously [20–22] using Powerup SYBR Green master mix (Thermo Fisher Scientific, Waltham, MA, USA). The primer sequences were as follows: IFN-γ, forward GGAGAGAGGAGGGT GACAGA and reverse TTGGATGCTCTGGTTGTCTT TA; IL-6, forward GATTCAATGAGGAGACTTGCC and reverse TGTTCTGGAGGTACTCTAGGTA.

**Table 1** Pathological evaluation and scoring system

| | |
|---|---|
| Total inflammation/gliosis | |
| 0 | No inflammation/gliosis |
| 1 | Minimal inflammation/gliosis |
| 2 | Mild inflammation/gliosis |
| 3 | Moderate inflammation/gliosis |
| 4 | Marked inflammation/gliosis |
| Inflammatory cuffing | |
| 0 | No inflammation present |
| 1 | Rare (1–3) perivascular cuffs/average whole section |
| 2 | Moderate numbers (4–10) of perivascular cuffs/sections; possible meningeal inflammation |
| 3 | Widespread perivascular cuffing and parenchymal infiltration by inflammatory cells |
| Demyelination | |
| 0 | No demyelination present |
| 1 | Rare demyelination foci |
| 2 | Multiple small demyelination foci |
| 3 | Multiple larger demyelination foci |
| 4 | Large confluent areas of demyelination |
| Activated microglial cells (MRP-$14^+$) | |
| 0 | No activated microglial cells |
| 1 | Minimal numbers of activated microglial cells |
| 2 | Mild numbers of activated microglial cells |
| 3 | Moderate numbers of activated microglial cells |
| 4 | Marked numbers of activated microglial cells |
| Percentage of $CD3^+$ or MRP-$14^+$ cells in cuffs | |
| 0 | No $CD3^+$ or MRP-$14^+$ cells |
| 1 | 0–25% of cells |
| 2 | 26–50% of cells |
| 3 | 51–75% of cells |
| 4 | > 75% of cells |
| $CD3^+$ or MRP-$14^+$ cells throughout parenchyma | |
| 0 | No $CD3^+$ or MRP-$14^+$ cells |
| 1 | Rare $CD3^+$ or MRP-$14^+$ cells |
| 2 | Mild numbers of $CD3^+$ or MRP-$14^+$ cells |
| 3 | Moderate numbers of $CD3^+$ or MRP-$14^+$ cells |
| 4 | Marked, widespread infiltrates of $CD3^+$ or MRP-$14^+$ cells |

## Detection of Anti-MOG Antibody

ELISA plates were coated with $rhMOG_{1–125}$ protein at 100 ng/well in PBS overnight at 4 °C and blocked with casein blocking buffer (Sigma) for 1 h at 37 °C. Marmoset plasma samples (diluted at 1:1000) were added to the wells and plates were incubated for 2 h at room temperature. Bound antibody was detected using horseradish peroxidase-conjugated goat anti-human IgG antibody (Thermo Fisher Scientific, San Jose, CA, USA) and 3,5,3′,5′-tetramethylbenzidine (Sigma).

### Statistical Analysis

The survival curve was evaluated with a log-rank (Mantel-Cox) test and other data were analyzed with the two-tailed unpaired Student's *t* test using GraphPad Prism software. A *p* value less than 0.05 was considered statistically significant.

## Results

### Development of EAE and Survival

Here, we used marmoset EAE as a model of MS, because MD-3 can recognize only human or nonhuman primate ICAM-1 molecules. Ten marmosets were initially immunized with human MOG protein and subsequently treated with either vehicle (PBS, $n = 5$) or MD-3 ($n = 5$) (Fig. 1a). Nine of the ten marmosets developed overt neurological signs of EAE, reaching clinical scores up to 2.5. One animal (no. 2002) in the MD-3 group persistently scratched the immunization site and failed to develop EAE until 46 days after immunization and thus was excluded from the present analysis. The clinical course for each animal is shown in Fig. 1b.

The nine marmosets with overt clinical symptoms of EAE showed rapidly progressive clinical deterioration to humane endpoints or death, exhibiting lethargy, anorexia, tail paralysis, and tremors. MD-3 treatment delayed the development of EAE fairly well and thereby extending the survival time (Fig. 1b, c). When evaluated based on EAE progression rate, which was defined as the interval between the day of MOG inoculation and the first day when a clinical score of 2 was achieved [17], the range for the vehicle group was 24–46 days (mean 35.2 days) and that for the MD-3 group was 36–77 days (mean 52.5 days).

### Analysis of Brain Lesions

Prior to euthanization at the endpoint, the volume of white matter T2 lesions was analyzed with T2-weighted magnetic resonance images (Fig. 2). For the reasons described in the "Materials and Methods" section, MRI data was available from only six animals. Among these animals, two marmosets in the vehicle group and one in the MD-3-treated group showed large white matter T2 lesions, although statistically significant differences did not exist within the two groups (Table 2).

All animals were euthanized at the stage of clinically evident EAE and histopathological analysis was performed ($n = 5$ for vehicle and $n = 4$ for MD-3). Pathologic findings observed in animals from both groups were consistent with rhMOG-induced EAE in marmosets [23]. Specifically, there was perivascular infiltration of mononuclear inflammatory cells (perivascular cuffs) accompanied by either multifocal or coalescing regions of demyelination and gliosis (Fig. 3a, b). $CD3^+$ T cells were variably present in the perivascular cuffs and these cells extended into the neural parenchyma (Fig. 3c). $MRP\text{-}14^+$ microglial cells were scattered in the perivascular cuffs and this type of cells was dominant within the areas of inflammation and gliosis in the parenchyma (Fig. 3d). The microglial cells had two different types of morphology consistent with either nonactivated or activated cells. Relatively severe lesions were observed in the cerebral cortex and striatum (white matter), diencephalon (white matter), and pons and medulla oblongata (white matter) regions (Table 3). There was a clear MD-3 treatment-related reduction in all of the scores in the white matter of cerebral cortex and striatum. Especially, total inflammation/gliosis, activated microglial cells, demyelination score, $CD3^+$ cell percentage in cuffs, and $MRP\text{-}14^+$ cell percentage in the parenchyma showed statistically significant reduction in MD-3-treated marmosets compared with the vehicle group, suggesting that MD-3 treatment could efficiently suppress T cell-mediated cellular immune reaction in the marmoset EAE model.

Next, we examined whether the histopathologic features of each animal were compatible with the MRI findings. Histopathologic analysis of three animals (no. 1001, no. 1003, and no. 2003) that showed large white matter T2 lesions (9.34, 14.16, and 8.17%, respectively) in MRI revealed moderate to severe inflammation and demyelination in the brain (inflammation/demyelination scores = 4/4, 4/3, and 2/2, respectively). In contrast, two MD-3-treated animals (no. 2004 and no. 2005) showed only minimal or mild pathologic lesions in MRI (white matter lesion = 0.18 and 0.29%, respectively) as well as histopathologic analysis (inflammation/demyelination scores = 0/0 and 1/0, respectively). Only one animal in the vehicle group (no. 1002) showed discrepancies between the MRI white matter lesion (0.23%) and the histopathologic inflammation and demyelination scores (4/3).

To further validate the differences in the histopathological findings for the two groups, IFN-γ and IL-6 transcript levels in the brain were measured using RT-qPCR. IFN-γ is a prototype cytokine produced by Th1 and CD8 T cells, and IL-6 is a potent inducer of the inflammatory response. These two types of cytokines have been known to increase in both multiple sclerosis [24] and marmoset EAE [21]. As expected, the transcript levels for both cytokines were lower in the MD-3-treated animals compared with the vehicle group (mean of vehicle vs. MD-3 group; IFN-γ = 0.059 vs. 0.013, IL-6 = 0.026 vs. 0.005) (Fig. 4). Considering the previous findings that MD-3 suppressed T cell activation and consequently the T cell-mediated immune response in xenotransplantation [14, 15] and collagen-induced arthritis [16], the results of histopathological and RT-qPCR analyses suggested that MD-3 delayed the development of EAE in marmoset monkeys via suppression of the T cell-mediated autoimmune reaction.

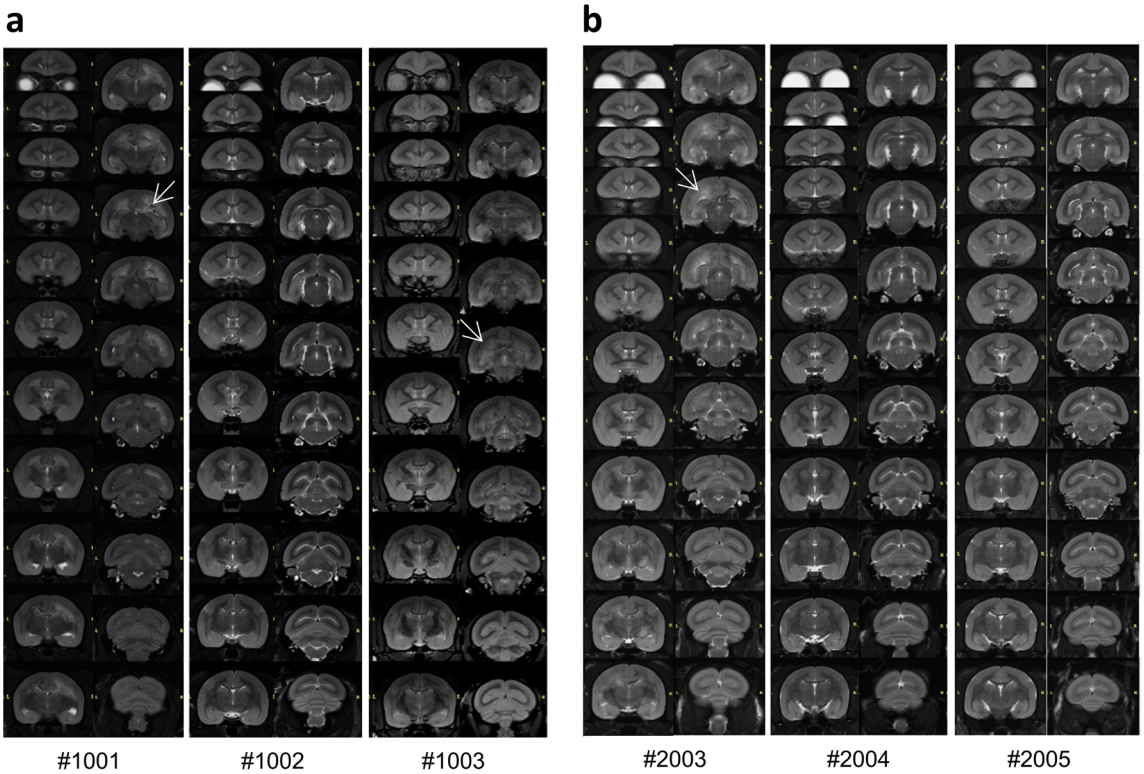


**Fig. 2** MRI white matter lesions in each marmoset. White matter T2-hyperintense EAE lesions (arrows) were induced in both **a** vehicle and **b** MD-3-treated animals. The treatment effect was not evidenced in MRI

## Serologic Analysis

To assess whether MD-3 treatment could suppress B cell response against immunized antigens, plasma samples were collected from each animal just prior to necropsy and were used for anti-MOG antibody assay. As summarized in Table 4, there was no significant difference in anti-MOG antibody concentration between the vehicle and MD-3 treated groups.

To evaluate whether the MD-3 antibody itself is immunogenic, the titers for MD-3 antibody and anti-MD-3 antibody were checked in plasma samples collected during necropsy. Notably, a substantial amount of MD-3 antibody remained in the plasma of MD-3-treated marmosets. We did not observe anti-MD-3 antibody in all of the animals (Table 4).

## Discussion

The ideal method for treating autoimmune diseases is the restoration of self-tolerance. Through many years of investigation via in vivo as well as in vitro studies, MD-3 has been identified as a novel form of anti-ICAM-1 antibody that recognizes different epitopes from previously identified sites. Engagement of this site with the MD-3 antibody is known to

**Table 2** MRI white matter lesion volumes

| Group | Marmoset no. | Whole brain vol. ($mm^3$) | Intact white matter volume ($mm^3$) | White matter lesion volume ($mm^3$) | % intact white matter | % white matter lesion |
|---|---|---|---|---|---|---|
| Vehicle | 1001 | 6715 | 853 | 627 | 12.70 | 9.34 |
| | 1002 | 7251 | 1193 | 17 | 16.45 | 0.23 |
| | 1003 | 7446 | 620 | 1054 | 8.33 | 14.16 |
| | Mean ± SD | 7137 ± 379 | 889 ± 288 | 566 ± 521 | 12.49 ± 4.07 | 7.91 ± 7.07 |
| MD-3 | 2003 | 7731 | 965 | 632 | 12.48 | 8.17 |
| | 2004 | 7307 | 1197 | 13 | 16.38 | 0.18 |
| | 2005 | 6920 | 1090 | 20 | 15.75 | 0.29 |
| | Mean ± SD | 7319 ± 406 | 1084 ± 116 | 222 ± 355 | 14.87 ± 2.09 | 2.88 ± 4.59 |
| *p* value | | 0.700 | 0.400 | 0.700 | 0.900 | 0.400 |

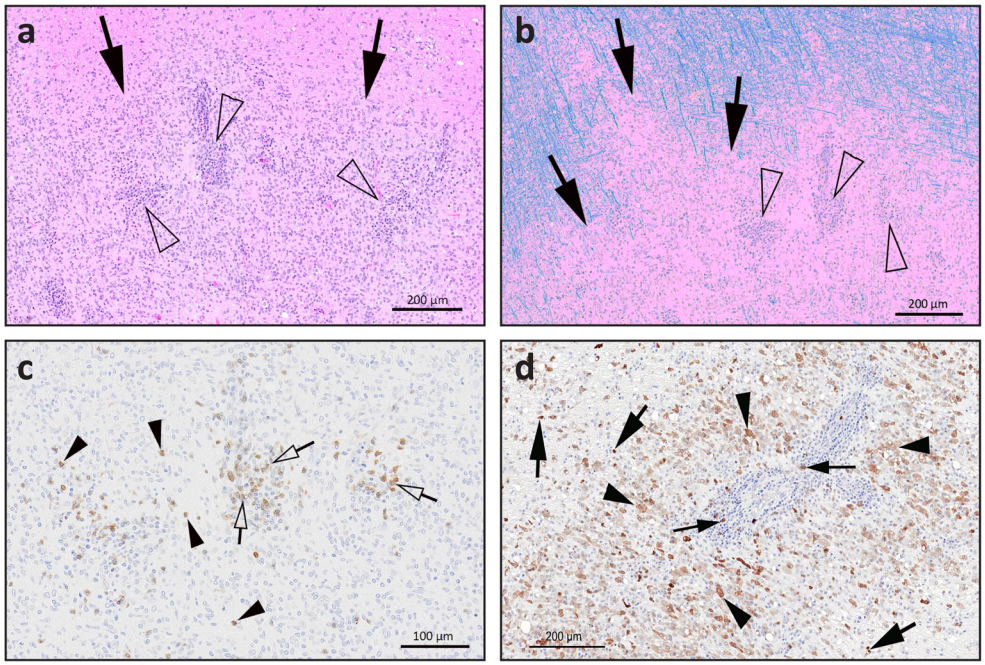


**Fig. 3** Histopathological features of rhMOG-immunized marmoset EAE. **a** Section of the cerebral cortex of the vehicle group brain (no. 1001), harvested at 44 days after rhMOG immunization, demonstrates extensive inflammation and gliosis (arrows; total inflammation/gliosis score 4) with several perivascular cuffs evident (open arrowheads; inflammatory cuffing score 3). **b** Luxol fast blue staining of same region of inflammation and gliosis demonstrates extensive loss of blue staining due to demyelination (arrows; demyelination score 4) around perivascular cuffs (open arrowheads). **c** On immunohistochemical staining for CD3 (same region as **a** and **b**), $CD3^+$ T cells are evident in both perivascular cuffs (open arrows; $CD3^+$ cell % score in cuffs 3) and throughout the region of inflammation and gliosis (arrowheads; $CD3^+$ cell % score in parenchyma 2). **d** Immunohistochemical staining for MRP-14 (same region as **a** and **b**) demonstrates large numbers of MRP-$14^+$-activated microglia (arrowheads; activated microglial cell score 4), as well as non-activated microglia (large arrows; MRP-$14^+$ cell % score in parenchyma 3), although MRP-$14^+$ cells are scarce in perivascular cuffs (small arrows; MRP-$14^+$ cell % score in cuffs 1)

**Table 3** Comparison of inflammation, demyelination, and T and microglial cell infiltrates between the vehicle and MD-3-treated groups

| | Total inflammation/ gliosis | Inflammatory cuffing score | Activated microglial cells | Demyelination score | % $CD3^+$ cells (cuffs) | % MRP-$14^+$ cells (cuffs) | % $CD3^+$ cells (parenchyma) | % MRP-$14^+$ cells (parenchyma) |
|---|---|---|---|---|---|---|---|---|
| Cerebral cortex and striatum/white matter | | | | | | | | |
| Vehicle | 3.8 ± 0.4[a] | 2.8 ± 0.4 | 3.8 ± 0.4 | 3.4 ± 0.5 | 2.4 ± 0.5 | 1.2 ± 0.4 | 2.0 ± 0.7 | 3.4 ± 0.5 |
| MD-3 | 1.5 ± 1.3 | 1.3 ± 1.5 | 1.5 ± 1.3 | 1.3 ± 1.5 | 0.5 ± 0.6 | 0.5 ± 0.6 | 1.0 ± 1.2 | 1.5 ± 1.3 |
| *p* value | 0.024 | ≥ 0.05 | 0.024 | 0.032 | 0.008 | ≥ 0.05 | ≥ 0.05 | 0.032 |
| Diencephalon/white matter | | | | | | | | |
| Vehicle | 3.2 ± 1.3 | 2.6 ± 0.9 | nd | 3.2 ± 1.3 | 2.6 ± 0.5 | nd | 1.8 ± 0.8 | nd |
| MD-3 | 2.8 ± 1.5 | 2.0 ± 1.2 | nd | 2.0 ± 1.4 | 1.8 ± 0.5 | nd | 1.5 ± 1.0 | nd |
| *p* value | ≥ 0.05 | ≥ 0.05 | | ≥ 0.05 | ≥ 0.05 | | ≥ 0.05 | |
| Pons and medulla oblongata/white matter | | | | | | | | |
| Vehicle | 3.2 ± 1.3 | 2.4 ± 0.9 | nd | 3.2 ± 1.3 | 2.2 ± 0.8 | nd | 1.4 ± 1.1 | nd |
| MD-3 | 2.5 ± 1.9 | 1.8 ± 1.8 | nd | 2.0 ± 1.4 | 1.5 ± 1.0 | nd | 1.8 ± v1.5 | nd |
| *p* value | ≥ 0.05 | ≥ 0.05 | | ≥ 0.05 | ≥ 0.05 | | ≥ 0.05 | |
| Spinal cord | | | | | | | | |
| Vehicle | 2.4 ± 1.1 | 2.0 ± 1.2 | 1.8 ± 1.5 | 1.8 ± 1.6 | 1.8 ± 1.1 | 1.4 ± 0.9 | 1.0 ± 0.0 | 2.0 ± 1.2 |
| MD-3 | 2.5 ± 1.0 | 1.8 ± 1.0 | 2.3 ± 1.0 | 2.5 ± 1.0 | 1.5 ± 0.6 | 1.0 ± 0.0 | 1.3 ± 0.5 | 2.3 ± 1.0 |
| *p* value | ≥ 0.05 | ≥ 0.05 | ≥ 0.05 | ≥ 0.05 | ≥ 0.05 | ≥ 0.05 | ≥ 0.05 | ≥ 0.05 |

*nd* not done

[a] Mean ± SD

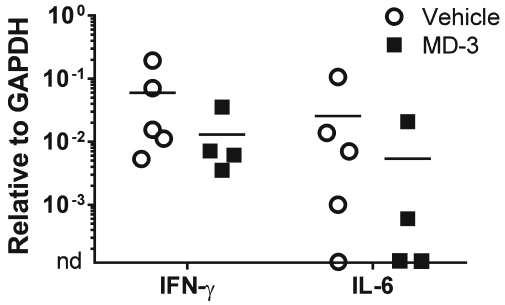


**Fig. 4** IFN-γ and IL-6 transcript expression level in the marmoset brain. mRNA was extracted from the cerebral hemispheres of marmosets, and the gene expression level was determined with RT-qPCR. Data is expressed relative to the household gene GAPDH. The MD-3-treated animals showed lower transcript levels for both IFN-γ and IL-6 compared with the vehicle group, although the difference was not statistically significant. nd, not detected

induce T cell tolerance or unresponsiveness to grafted xenoantigens [14, 15]. The efficacy of MD-3 has been replicated in cynomolgus monkeys with CIA, with respect to the number of affected joints and the severity of arthritis [16]. This study provided good evidence that MD-3 treatment greatly suppresses T cell and microglial infiltration as well as IFN-γ and IL-6 production in the brain. The major characteristics of EAE are induced by full-blown inflammation with resistance to a variety of therapeutic protocols. This factor seems to play a role in the inability to completely prevent disease development with MD-3, as was the case in CIA and porcine islet transplantation.

The initial step for the induction of MS and EAE is CD4 T cell priming by dendritic cells, which take up myelin antigens such as MOG, MBP, and PLP [6, 25, 26], subsequently followed by epitope spreading that causes long-term disease progression [6–8, 27]. The primary event in the rhMOG-induced marmoset model is the activation of Th1 cells against $MOG_{24–36}$ peptides, inducing small inflammatory lesions in the brain [17, 28, 29]. Other contributing factors are the generation of anti-MOG antibodies in the B cell compartment and activation of Th17 cells, both of which seem to amplify MS-like lesions [28, 30, 31]. In previous studies, we demonstrated that MD-3 suppressed in vitro development of human dendritic cells and induced antigen-specific T cell tolerance in humanized mice in a dendritic cell-dependent manner [14]. In addition, prophylactic treatment of MD-3 in a nonhuman primate transplantation model induced near-complete T cell unresponsiveness against grafted antigens [14, 15]). However, it seems that MD-3 is not as effective in suppressing pre-activated T cell responses. In the current study, MD-3 was administered 7 days after immunization with rhMOG proteins and therefore might have played its suppressive role mainly in T cell activation against autoantigens released after MD-3 administration, rather than during the initial T and B cell activation steps against immunized rhMOG proteins. During the initial 7 days before MD-3 injection, pathologic B cells could have already been activated and subsequently differentiated into plasma cells with the help of rhMOG-reactive T cells. This was evidenced by the detection of MOG antibodies in both vehicle-treated and MD-3-treated animals. It is well known that the antibody response by B cells can be effectively suppressed by CD40-CD40L blockade [32], and a group of professional investigators reported that blocking CD40-CD40L (CD154) interaction was effective at EAE prevention [33].

**Table 4** Anti-rhMOG, MD-3, and anti-MD-3 antibody concentration in plasma

| Animal no. | Day of sampling | MD-3 treatment | | Anti-rhMOG Ab (OD) | MD-3 (μg/ml) | Anti-MD-3 Ab |
|---|---|---|---|---|---|---|
| | | Number of doses | Length of time since the last dose (days) | | | |
| Vehicle | | | | | | |
| No. 1001 | 44 | 0 | | 0.399 | nd | nd |
| No. 1002 | 48 | 0 | | 0.473 | nd | nd |
| No. 1003 | 36 | 0 | | 0.208 | nd | nd |
| No. 1004 | 25 | 0 | | 0.069 | nd | nd |
| No. 1005 | 32 | 0 | | 0.239 | nd | nd |
| Mean ± SD | | | | 0.278 ± 0.160 | | |
| MD-3 treated | | | | | | |
| No. 2001 | 38 | 6 | 2 | 0.382 | 54.0 | nd |
| No. 2003 | 41 | 6 | 5 | 0.277 | 8.9 | nd |
| No. 2004 | 59 | 9 | 2 | 0.559 | 2.7 | nd |
| No. 2005 | 78 | 11 | 7 | 0.470 | 82.3 | nd |
| Mean ± SD | | | | 0.422 ± 0.121 | | |
| *p* value | | | | *0.*286 | | |

*nd* not detected

In the present study, we evaluated the therapeutic efficacy of MD-3 in a rapidly progressive marmoset model. On a theoretical basis, modulation of dendritic cell maturation by MD-3 seems to contribute to the blocking of secondary epitope spread, which may suppress further T cell activation during chronic inflammation. With this in mind, we expect MD-3 treatment to be a more preferable therapeutic protocol for slowly progressing or relapsing-remitting EAE and MS. Combination therapy with CD40-CD40L blockade might also exhibit a synergistic effect on MD-3.

Finally, the titers for the MD-3 and anti-MD-3 antibodies were measured in plasma samples collected during necropsy. We found that individual variation was very high in the plasma concentration of MD-3. As shown in Fig. 1a, MD-3 was administrated repeatedly, and therefore, the plasma level of the MD-3 antibody was dependent on both the number of doses and the length of time since the last dose. Additionally, we think the possibility that anti-MD-3 antibody generation below the detection level could have caused the rapid clearing of MD-3 antibody especially in animal no. 2004 as well as no. 2003 compared with the other animals (no. 2001 and no. 2005) cannot be excluded. This possibility was also raised in a 10-week repeated dose pharmacokinetic study performed separately in cynomolgus monkeys, in which some animals showed rapid clearance of intravenously administrated MD-3 antibody following repeated dosing (data not published).

**Acknowledgements** Special thanks are due to professor Seong Hoe Park of Seoul National University College of Medicine for his innumerable contributions, including many helpful discussions and continued advice during all experimental processes as well as reading the entire manuscript and providing comments.

## Compliance with Ethical Standards

**Conflict of Interest** All authors report no conflict of interest.

## References

1. Lassmann H, Bruck W, Lucchinetti CF (2007) The immunopathology of multiple sclerosis: an overview. Brain Pathol 17:210–218
2. Lublin FD, Reingold SC, Cohen JA, Cutter GR, Sorensen PS, Thompson AJ, Wolinsky JS, Balcer LJ et al (2014) Defining the clinical course of multiple sclerosis: the 2013 revisions. Neurology 83:278–286
3. Kebir H, Kreymborg K, Ifergan I, Dodelet-Devillers A, Cayrol R, Bernard M, Giuliani F, Arbour N et al (2007) Human TH17 lymphocytes promote blood-brain barrier disruption and central nervous system inflammation. Nat Med 13:1173–1175
4. Zhang J, Markovic-Plese S, Lacet B, Raus J, Weiner HL, Hafler DA (1994) Increased frequency of interleukin 2-responsive T cells specific for myelin basic protein and proteolipid protein in peripheral blood and cerebrospinal fluid of patients with multiple sclerosis. J Exp Med 179:973–984
5. Farooqi N, Gran B, Constantinescu CS (2010) Are current disease-modifying therapeutics in multiple sclerosis justified on the basis of studies in experimental autoimmune encephalomyelitis? J Neurochem 115:829–844
6. Constantinescu CS, Farooqi N, O'Brien K, Gran B (2011) Experimental autoimmune encephalomyelitis (EAE) as a model for multiple sclerosis (MS). Br J Pharmacol 164:1079–1106
7. McRae BL, Vanderlugt CL, Dal Canto MC, Miller SD (1995) Functional evidence for epitope spreading in the relapsing pathology of experimental autoimmune encephalomyelitis. J Exp Med 182:75–85
8. Quintana FJ, Patel B, Yeste A, Nyirenda M, Kenison J, Rahbari R, Fetco D, Hussain M et al (2014) Epitope spreading as an early pathogenic event in pediatric multiple sclerosis. Neurology 83:2219–2226
9. Vanderlugt CL, Neville KL, Nikcevich KM, Eagar TN, Bluestone JA, Miller SD (2000) Pathologic role and temporal appearance of newly emerging autoepitopes in relapsing experimental autoimmune encephalomyelitis. J Immunol 164:670–678
10. Furuya K, Takeda H, Azhar S, McCarron RM, Chen Y, Ruetzler CA, Wolcott KM, DeGraba TJ et al (2001) Examination of several potential mechanisms for the negative outcome in a clinical stroke trial of enlimomab, a murine anti-human intercellular adhesion molecule-1 antibody: a bedside-to-bench study. Stroke 32:2665–2674
11. Kavanaugh AF, Davis LS, Nichols LA, Norris SH, Rothlein R, Scharschmidt LA, Lipsky PE (1994) Treatment of refractory rheumatoid arthritis with a monoclonal antibody to intercellular adhesion molecule 1. Arthritis Rheum 37:992–999
12. Salmela K, Wramner L, Ekberg H, Hauser I, Bentdal O, Lins LE, Isoniemi H, Backman L et al (1999) A randomized multicenter trial of the anti-ICAM-1 monoclonal antibody (enlimomab) for the prevention of acute rejection and delayed onset of graft function in cadaveric renal transplantation: a report of the European Anti-ICAM-1 Renal Transplant Study Group. Transplantation 67:729–736
13. Vuorte J, Lindsberg PJ, Kaste M, Meri S, Jansson SE, Rothlein R, Repo H (1999) Anti-ICAM-1 monoclonal antibody R6.5 (Enlimomab) promotes activation of neutrophils in whole blood. J Immunol 162:2353–2357
14. Jung KC, Park CG, Jeon YK, Park HJ, Ban YL, Min HS, Kim EJ, Kim JH et al (2011) In situ induction of dendritic cell-based T cell tolerance in humanized mice and nonhuman primates. J Exp Med 208:2477–2488
15. Lee JI, Kim J, Choi YJ, Park HJ, Park HJ, Wi HJ, Yoon S, Shin JS, Park JK, Jung KC, Lee EB, Kang HJ, Hwang ES, Kim SJ, Park CG, Park SH (2018) The effect of epitope-based ligation of ICAM-1 on survival and retransplantation of pig islets in nonhuman primates. Xenotransplantation 25:e12362
16. Lee JI, Park HJ, Park HJ, Choi YJ, Kim J, Park JK, Jung KC, Hwang ES et al (2018) Epitope-based ligation of ICAM-1: Therapeutic target for protection against the development of rheumatoid arthritis. Biochem Biophys Res Commun 500:450–455
17. Kap YS, Jagessar SA, van Driel N, Blezer E, Bauer J, van Meurs M, Smith P, Laman JD et al (2011) Effects of early IL-17A neutralization on disease induction in a primate model of experimental autoimmune encephalomyelitis. J NeuroImmune Pharmacol 6:341–353
18. Laman JD, 't Hart BA, Brok H, Meurs M, Schellekens MM, Kasran A, Boon L, Bauer J et al (2002) Protection of marmoset monkeys against EAE by treatment with a murine antibody blocking CD40 (mu5D12). Eur J Immunol 32:2218–2228
19. Yushkevich PA, Piven J, Hazlett HC, Smith RG, Ho S, Gee JC, Gerig G (2006) User-guided 3D active contour segmentation of anatomical structures: significantly improved efficiency and reliability. Neuroimage 31:1116–1128
20. Fujii Y, Kitaura K, Matsutani T, Shirai K, Suzuki S, Takasaki T, Kumagai K, Kametani Y et al (2013) Immune-related gene expression profile in laboratory common marmosets assessed by an

accurate quantitative real-time PCR using selected reference genes. PLoS One 8:e56296
21. Jagessar SA, Heijmans N, Blezer EL, Bauer J, Weissert R, 't Hart BA (2015) Immune profile of an atypical EAE model in marmoset monkeys immunized with recombinant human myelin oligodendrocyte glycoprotein in incomplete Freund's adjuvant. J Neuroinflammation 12:169
22. Jagessar SA, Vierboom M, Blezer EL, Bauer J, Hart BA, Kap YS (2013) Overview of models, methods, and reagents developed for translational autoimmunity research in the common marmoset (Callithrix jacchus). Exp Anim 62:159–171
23. Genain CP, Roberts T, Davis RL, Nguyen MH, Uccelli A, Faulds D, Li Y, Hedgpeth J et al (1995) Prevention of autoimmune demyelination in non-human primates by a cAMP-specific phosphodiesterase inhibitor. Proc Natl Acad Sci U S A 92:3601–3605
24. Gobel K, Ruck T, Meuth SG (2018) Cytokine signaling in multiple sclerosis: lost in translation. Mult Scler 24:432–439
25. 't Hart BA, Gran B, Weissert R (2011) EAE: imperfect but useful models of multiple sclerosis. Trends Mol Med 17:119–125
26. de Vos AF, van Meurs M, Brok HP, Boven LA, Hintzen RQ, van der Valk P, Ravid R, Rensing S et al (2002) Transfer of central nervous system autoantigens and presentation in secondary lymphoid organs. J Immunol 169:5415–5423
27. Vanderlugt CL, Miller SD (2002) Epitope spreading in immune-mediated diseases: implications for immunotherapy. Nat Rev Immunol 2:85–95
28. Brok HP, Uccelli A, Kerlero De Rosbo N, Bontrop RE, Roccatagliata L, de Groot NG, Capello E, Laman JD et al (2000) Myelin/oligodendrocyte glycoprotein-induced autoimmune encephalomyelitis in common marmosets: the encephalitogenic T cell epitope pMOG24-36 is presented by a monomorphic MHC class II molecule. J Immunol 165:1093–1101
29. Kap YS, Smith P, Jagessar SA, Remarque E, Blezer E, Strijkers GJ, Laman JD, Hintzen RQ et al (2008) Fast progression of recombinant human myelin/oligodendrocyte glycoprotein (MOG)-induced experimental autoimmune encephalomyelitis in marmosets is associated with the activation of MOG34-56-specific cytotoxic T cells. J Immunol 180:1326–1337
30. Genain CP, Nguyen MH, Letvin NL, Pearl R, Davis RL, Adelman M, Lees MB, Linington C et al (1995) Antibody facilitation of multiple sclerosis-like lesions in a nonhuman primate. J Clin Invest 96:2966–2974
31. Jagessar SA, Kap YS, Heijmans N, van Driel N, van Straalen L, Bajramovic JJ, Brok HP, Blezer EL et al (2010) Induction of progressive demyelinating autoimmune encephalomyelitis in common marmoset monkeys using MOG34-56 peptide in incomplete freund adjuvant. J Neuropathol Exp Neurol 69:372–385
32. Kelsoe G (2003) Therapeutic CD154 antibody for lupus: promise for the future? J Clin Invest 112:1480–1482
33. Boon L, Brok HP, Bauer J, Ortiz-Buijsse A, Schellekens MM, Ramdien-Murli S, Blezer E, van Meurs M et al (2001) Prevention of experimental autoimmune encephalomyelitis in the common marmoset (Callithrix jacchus) using a chimeric antagonist monoclonal antibody against human CD40 is associated with altered B cell responses. J Immunol 167:2942–2949